



Original Paper

Extensional structures of the Nan'an Basin in the rifting tip of the South China Sea: Implication for tectonic evolution of the southwestern continental margin



Shi-Guo Wu^{a, c, d, *}, Li Zhang^b, Zhen-Yu Lei^b, Xing Qian^b, Shuai-Bing Luo^b, Xiang-Yang Lu^a, Thomas Lüdmann^e, Lei Tian^f

^a Laboratory of Geophysics and Georeouce, Institute of Deep-sea Science and Engineering, China Academy of Science, Sanya, Hainan 572000, China

^b MLR Key Laboratory of Marine Mineral Resources, Guangzhou Marine Geological Survey, Guangzhou, Guangdong 510075, China

^c South Marine Science and Engineering Guangdong Laboratory (Zhuhai), Zhuhai, Guangdong 519000, China

^d University of China Academy of Sciences, Beijing 100049, China

^e Institute for Geology, CEN, University of Hamburg, Hamburg, 20146, Germany

^f Research Institute of Petroleum Exploration and Development Northwest Branch, Lanzhou, Gansu 730000, China

ARTICLE INFO

Article history:

Received 22 February 2022

Received in revised form

13 July 2022

Accepted 30 August 2022

Available online 6 September 2022

Edited by Teng Zhu and Jia-Jia Fei

Keywords:

Sedimentary basin

Seismic sequence

Rifting

Tectonic evolution

South China Sea

ABSTRACT

Nan'an Basin is a giant hydrocarbon basin, but its tectonic division scheme and associated fault systems has not been well understood. Based on newly acquired seismic data from the southwestern margin of the South China Sea, this study analyzed the structural units, tectonic feature and geodynamics of the sedimentary basin. The new data suggests that the Nan'an Basin is a rift basin oriented in the NE-SW direction, rather than a pull-apart basin induced by strike-slip faults along the western margin. The basin is a continuation of the rifts in the southwest South China Sea since the late Cretaceous. It continued rifting until the middle Miocene, even though oceanic crust occurred in the Southwest Sub-basin. However, it had no transfer surface at the end of spreading, where it was characterized by a late middle Miocene unconformity (reflector T3). The Nan'an Basin can be divided into eight structural units by a series of NE-striking faults. This study provides evidences to confirm the relative importance and interplay between regional strike-slips and orthogonal displacement during basin development and deformation. The NE-SW-striking dominant rift basin indicates that the geodynamic drivers of tectonic evolution in the western margin of the South China Sea did not have a large strike-slip mechanism. Therefore, we conclude that a large strike-slip fault system did not exist in the western margin of the South China Sea.

© 2022 The Authors. Publishing services by Elsevier B.V. on behalf of KeAi Communications Co. Ltd. This is an open access article under the CC BY license (<http://creativecommons.org/licenses/by/4.0/>).

1. Introduction

The western margin of the South China Sea (SCS) is thought to be formed by strike-slip movement offshore Vietnam (Tapponnier et al., 1982; Rangin et al., 1995; Yao et al., 2005; Savva et al., 2014). The strike-slip fault extends from the Red River Fault via the East Vietnam Fault and is connected to the Lupar Fault to the south (Morley, 2002; Liu et al., 2004; Qiu et al., 2005; Yao et al., 2005). A giant strike-slip component that occurred in the

Cenozoic could be an important mechanism that induced the opening of the South China Sea (Tapponnier et al., 1982). The pull-apart basin, Wan'an (Nam Con Son) Basin, was formed by the strike-slip fault (Yao et al., 2008, 2018). However, some other studies have argued that the strike-slip fault did not have a large strike-slip component during the Cenozoic because no apparent strike-slip movement occurred during the Tertiary (Clift et al., 2008; Cullen et al., 2010; Sun et al., 2011; Franke et al., 2014; Morley, 2016).

Nan'an Basin, including Wan'an (Nam Con Son) and part of the Nanwei Basin, is located at the tip of the Southeast Subbasin in the South China Sea (Fig. 1a). It is a distal rifting basin that connects to the continental-ocean boundary (COB) (Hall, 2002; Ding et al., 2013; Gao et al., 2016; Yao et al., 2018; Song et al., 2019). Similar

* Corresponding author. Laboratory of Geophysics and Georeouce, Institute of Deep-sea Science and Engineering, China Academy of Science, Sanya, Hainan 572000, China.

E-mail address: swu@idsse.ac.cn (S.-G. Wu).

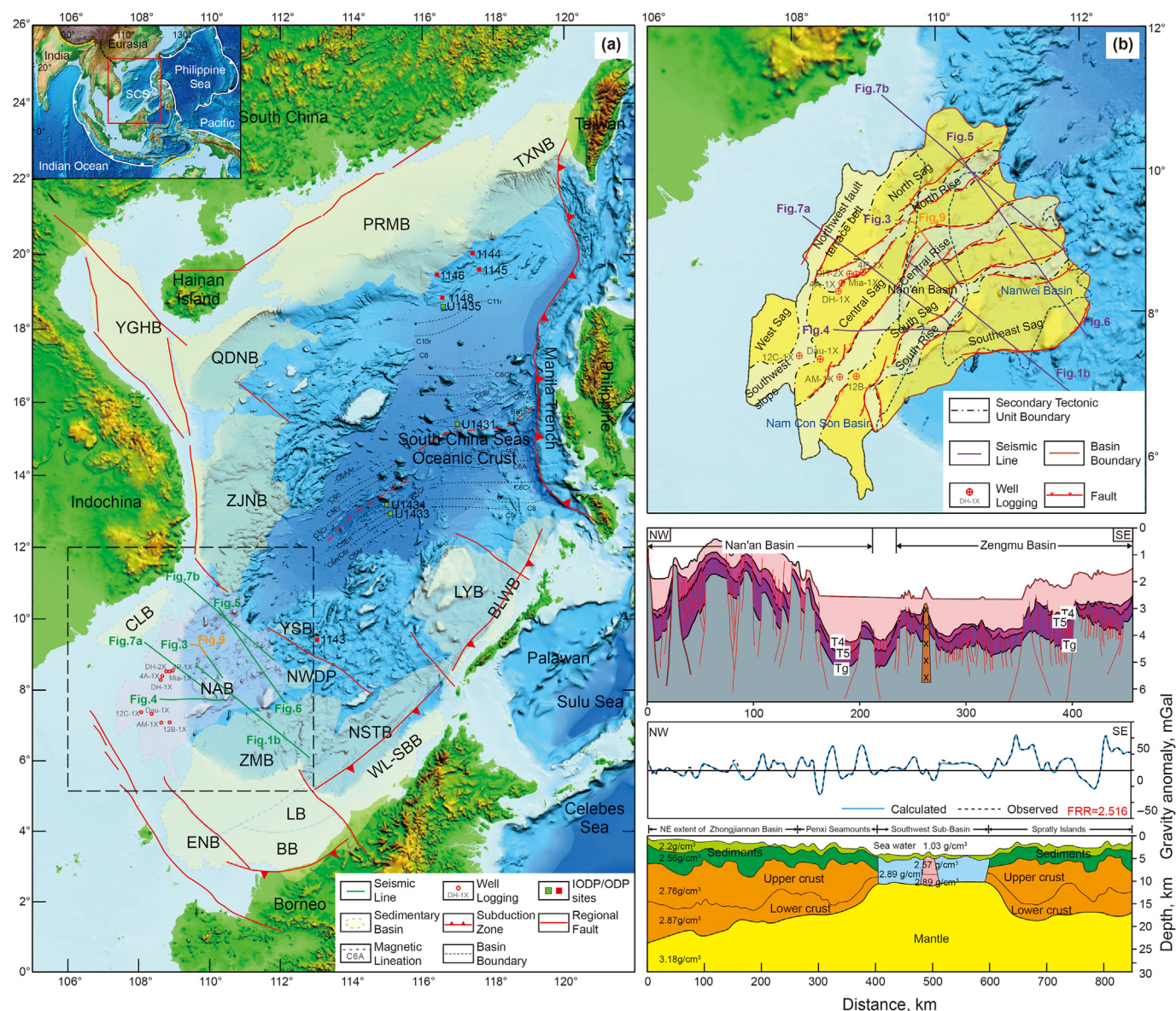


Fig. 1. (a) Tectonic location of Nan'an Basin, South China Sea. The upper left inset shows the regional plate tectonics of the SCS. The lower right legend is illustrations of the main geologic symbols. The squares are the IODP/ODP sites. BB is Balingan Basin, CLB is Cuu Long Basin, ENB is East Natuna Basin, LB is Luconia Basin, LYB is Lijue Basin, NAB represents Nan'an Basin, PRMB is Pearl River Mouth Basin, QDNB is Qiongdongnan Basin, TXNB is Taixinan Basin, YGHB is Yinggehai Basin, and ZMB represents Zengmu Basin. The box indicates the location of the Nan'an Basin. The red solid lines indicate the major faults; (b) is structural units of Nan'an Basin, the geological section across the Southwest Subbasin and Nansha Block of the south margin. The top shows structural units of Nan'an Basin and the seismic track line positions mentioned in the text. Circles with a cross indicate drilling well sites, purple lines indicate the locations of the seismic sections, red lines represent the faults, dot-dashed lines represent boundary of the second units of the sedimentary basin, and the blue dashed line outlines the original Nam Con Son Basin (Matthews et al., 1997) and Nanwei Basin (Yao et al., 2005); Lower is the structural section across the Zengmu Basin and Nan'an Basin, and see Fig. 1a for location. Bottom is the comprehensive profile across the Southwest Subbasin (Qiu et al., 2005).

to several deepwater basins (Zhang et al., 2019; Zhu et al., 2022), this basin is rich in oil and gas, and several geophysical survey cruises have been conducted since the 1980s (Matthews et al., 1997; Yao et al., 2008; Cullen et al., 2010). Based on the geophysical data, many geologists suggest that the basin was a strike-slip basin that formed since the Eocene (Cliff et al., 2008; Yao et al., 2008). However, new geophysical surveys executed by the GMGS (Guangzhou Marine Geological Survey) indicate that the basin may extend eastward to the Southwest Subbasin. Initial rifting sequences existed during the late Cretaceous and early Eocene, but no typical NS-striking slip fault controlled the basin boundary. Furthermore, there are NE-striking rift faults controlled the main depressions of the Nan'an Basin (Matthews et al., 1997; Morley, 2002). Therefore,

the Nan'an Basin have been a NE-striking rift basin since the Paleocene (Wu et al., 2016). It was the continuation of the Southwest Subbasin SCS during the rifting stage.

The Nan'an Basin is a key oil-bearing province to be confirmed if it is a large strike-slip fault dominated pull apart basin or a rifting basin. In this study, we studied the structural units, evolution of the main fault, and geodynamics of the Nan'an Basin using newly acquired seismic data. Furthermore, we discussed the Neogene tectonic evolution of the western margin of SCS.

2. Geological setting

Nan'an Basin is located at the tip of the Southwest Subbasin in

the SCS, adjacent to the Indo-China Peninsula of the Eurasian Plate, which includes the Wan'an Basin (Nam Con Son Basin) (Fig. 1b) (Matthews et al., 1997; Lee et al., 2001; Yao et al., 2008) and the part of Nanweixi Basin (Peng et al., 2019; see also in Fig. 1b). The basin extends from the continental shelf to the slope, and the maximum water depth reaches 1800 m. The basement of the Nan'an Basin is composed of Hercynian-Indosinian metamorphosed rocks and the Yanshan volcanic arc (Yan et al., 2014). However, middle Jurassic to late Cretaceous granite and diorite (178 ± 5 Ma– 97 ± 3 Ma) were encountered in more than 20 drilling wells in the sedimentary basin. The rift sequence of the Nan'an Basin is older than that of Cuu Long Basin (Fig. 1a), but previous articles have taken unexpected different views of Neogene tectonic movement (Matthews et al., 1997; Lü et al., 2013). The early Oligocene extension in the Cuu Long Basin was relatively weak, with little expansion during the Oligocene fault period. However, at least two Neogene rifting stages occurred in Nan'an Basin, which underwent lateral extension (Yao et al., 2005), especially during the middle Miocene extension as imaged by the seismic profiles. Breakup unconformities are widely distributed during early Oligocene. The middle Miocene (10.5 Ma) unconformity marked the tectonic inverse of significant middle Miocene rifting. Although the lower Miocene Wan'an Formation was considered post-rifting sequence, the last phase of rifting was identified in the middle Miocene Lizhun Formation and late Miocene Kunlun Formation between 15.5 and 10.5 Ma. The last rifting phase unconformity occurred in latest Miocene (Fig. 2). This means that the main rifting phase lasted from the Eocene to the middle Miocene. Interestingly, all the structures were active in reflector T₃. The Nan'an Basin experienced post-rift subsidence in the early Miocene, followed by extension from the middle Miocene to 10.5 Ma, and then ended.

3. Cenozoic sequence stratigraphy

3.1. Seismic reflectors and unconformities

Based on the seismic interpretation of the Nan'an Basin, seven seismic reflectors have been discerned in the basin: seismic reflectors T₁, T₂, T₃, T₃¹, T₄, T₅ and T_g (Wu et al., 2016; Yao et al., 2005; Lunt, 2019; see also Figs. 2–7). The stratigraphic division initial referred to Wu (1997). Recently, Dung et al. (2018) redefined the reflectors based on the drilling wells. Reflector T₁ reflected the unconformity and relative conformity induced by eustasy curve. It represents the boundary (1.8 Ma) between Quaternary and Pliocene. Reflector T₂ is widely unconformity in the Nan'an Basin. It was named Guangya event (Yao et al., 2008) and corresponded to 5.3 Ma. Reflector T₃ was an important unconformity in the Nan'an Basin, and represented the beginning of collision between the Borneo and Nansha Block. Reflector T₃¹ was the spreading end of the Southwest Subbasin at 16.5 Ma. Maybe the tectonic postpone led to occurrence of local unconformity. Reflector T₄ represented the breakup of the Southwest Subbasin which has great effect on the Nan'an Basin. It was encountered by drilling wells, and its age was 23.3 Ma between Oligocene and early Miocene. Reflector T₅ and T_g beneath the reflector T₄ has no drilling well control, but shows strong reflection on the seismic profiles (Figs. 3–7).

The reflector T₁ unconformity represents the boundary between the Quaternary and Pliocene. It occurred within the sedimentary depression and varied in thickness from the shelf to the slope basin. It was characterized by typical foreset cross-bedding sequences and by high frequencies, large amplitudes, and continuity. A deep-water channel system occurs in a local slope canyon that is parallel to the Southwest Subbasin.

Reflector T₂ corresponds to the boundary between the Pliocene and upper Miocene. Reflector T₂ has a large amplitude and good

continuity in the continental shelf. It was characterized by two sets of reflection waves in the continental slope which have moderate amplitudes, low to middle frequencies, and are very continuous. The sequence varied from continental shelf to slope facies and was characterized by onlap in the basin margin due to rising sea level.

Reflector T₃ is an important unconformity between the upper and middle Miocene, and may be related to the Borneo orogeny (Maddon et al., 2013). It has moderate to large amplitudes and good continuity and local overlap in the depression of the basin, whereas it shows weak amplitudes and discontinuity in the uplift.

Reflector T₃¹ is the boundary between the middle and lower Miocene. The entire basin was discernible and it became an important unconformity. The reflector has a large amplitude and good continuity. The seismic sequence over the reflector has a parallel reflection, few faults, and weak deformation. However, the seismic sequence below the reflector shows intense deformation.

Reflector T₄ has been argued over. A few studies consider that it could be a breakup unconformity. However, we suggest that reflector T₄ indicates the response to the opening of the Southwest Subbasin in the early Miocene. Reflector T₄ has low to moderate frequencies, moderate and large amplitudes, and continuous reflections. It is weaker and more variable in magnitude and becomes indistinct at the centre of the depression. The low-frequency sequences below the reflector onlap to the basin slope and belong to the rifting fill sequences.

Reflector T₅ is the breakup unconformity between the boundary of the upper and middle Eocene. Reflector T₅ can be traced through the entire basin. It has an apparent unconformity with low-frequency, high-amplitudes, and continuous reflections. It mixed with the T_g reflector during the uplift.

Reflector T_g is interpreted as the acoustic basement of the basin, which reflects the transfer from compression uplift to rifting in the Indo-China Peninsula. Reflector T₅ experienced long-term erosion; hence, reflectors T_g and T₅ are mixed together. Reflector T_g had various amplitudes and continuity reflections, and diffraction waves occurred in the rise. It showed fuzzy and faulted reflections and was difficult to trace due to the poor seismic quality.

3.2. Cenozoic seismic stratigraphy

Based on the seismic profiles across Nan'an Basin and drilling results from Wells 12C-1X, 12B-1X, Dua-1X, AM-1X, DH-1X, DH-2X, 4A-1X, Mia-1X, and 4B-1X, seven seismic reflectors, namely, T₁, T₂, T₃, T₃¹, T₄, T₅, and T_g, were identified. Eight regional seismic sequences have been divided by these seismic reflectors since the Eocene. The Cenozoic strata have been divided into the Renjun, Xiwei, Wan'an, Lizhun, Kunlun, and Guangya Formations from the bottom to the top (Fig. 8). The maximum depth of Well Dua-1X revealed that the thicknesses of the Xiwei, Wan'an, Lizhun, Kunlun, and Guangya Formations are 915 m, 415 m, 830 m, 275 m, and 990 m, respectively. The seismic sequence between reflectors T₅ and T_g was not encountered in the drilling well, and is called the Renjun Formation (Yao et al., 2005, see also Figs. 3–7).

The acoustic basement may be Mesozoic metamorphic rock and granite (Matthews et al., 1997; Liu et al., 2004). The lowest Renjun Group is the initial rifting sequence over the acoustic basement. The strata between reflectors T₅ and T_g were inferred to be lower and middle Eocene strata. The sequences have moderate to high amplitudes, moderate frequencies, and discontinuous reflections. Its external form has a wedge shape and is interpreted as half-graben fillings. We infer that the lithology is terrestrial alluvial, fluvial, and lacustrine facies, and contains glutenite and few fossils. It was limited to the deep depression of Wan'an Basin over the unconformity. The maximum depth of SQ1 was less than 1000 m in the eastern basin.

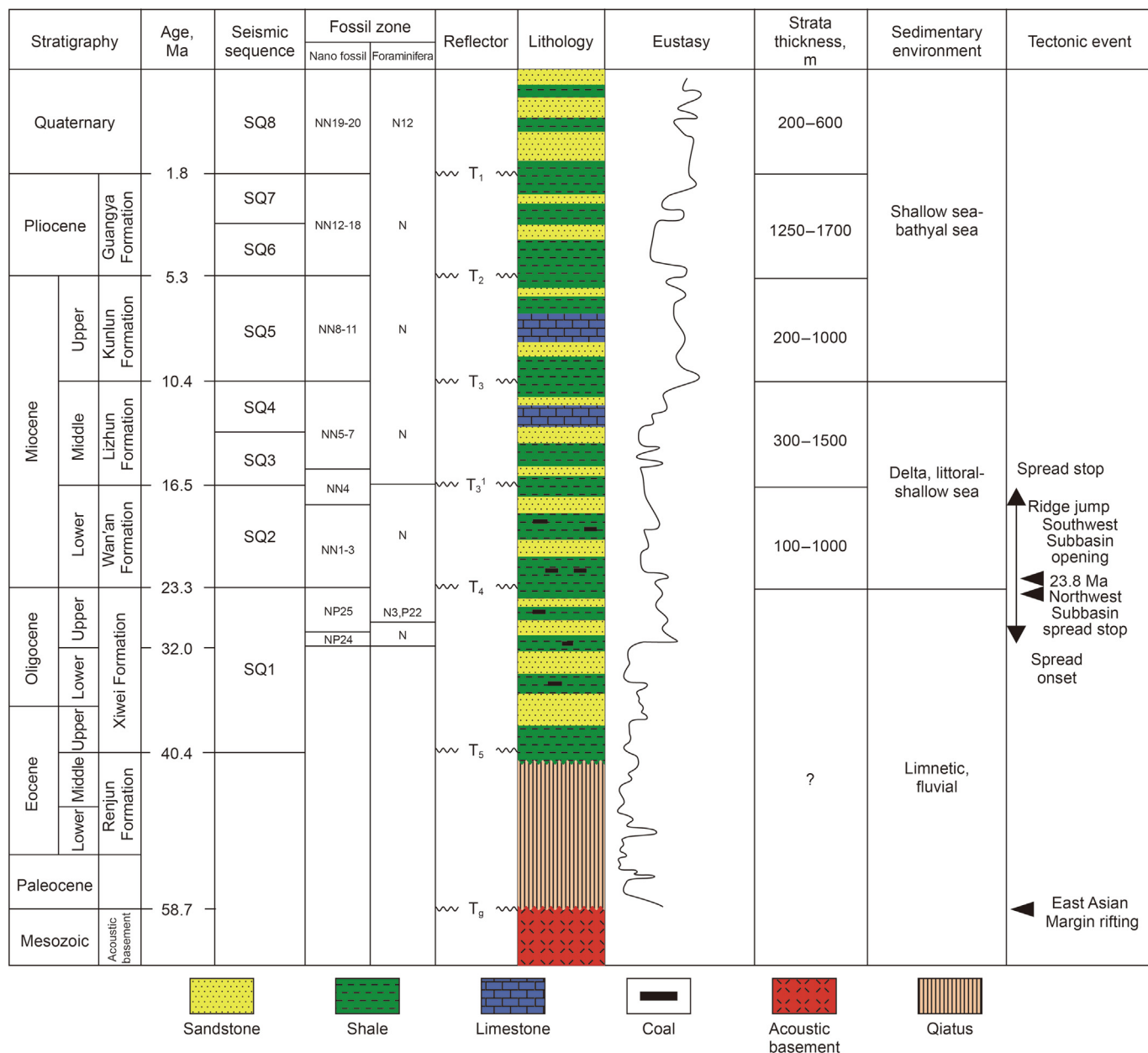


Fig. 2. Generalized columnar section showing the stratigraphy and seismic sequence in Nan'an Basin, South China Sea. Eight sequences since the late Eocene have been identified in Nan'an Basin. The sea level curve was obtained from Haq et al. (1987). Cenozoic sedimentary facies in Nan'an Basin varied from terrestrial to deep marine. The tectonic event and main unconformities referred from Taylor and Hayes (1980), Barckhausen et al. (2014), Li et al. (2014a) and Lunt (2019).

SQ1 is the Xiwei Formation, which is characterized by moderate to high amplitudes, moderate continuity or discontinuity, and weak frequency. It has an apparent onlap and varies in thickness 200–4000 m. The lacustrine facies were deposited in the northwest region of the basin. A few transitional facies occurred in the east of the basin, indicating that the transgressive facies came from the east. Well Dua-1X encountered SQ1 as a lacustrine interbedded sandstone and mudstone that contains a coalbed and bioclastics. The sequence fining upward and can be divided into a lowerstand fluvial channel, deltaic glutenite, transgressive shallow lacustrine mud, and a highstand deltaic floodplain.

SQ2 is the lower Miocene Wan'an Formation sequence between reflectors T₄ and T₃¹. The seismic reflection was characterized by moderate amplitudes, moderate continuity, parallel or diverge configuration, and a wedge-like shape. The reflections varies from

strong to weak amplitude from east to west. The top of the sequence shows truncation, onlap, downlap, and concordance. SQ2 was widely distributed throughout the basin, with a thickness of 400–2800 m. The sedimentary centre is located in the north of the sag. The sequence is usually 400–800 m, with a maximum thickness of 2000–2800 m.

In the late Oligocene, Nan'an Basin was dominated by shallow sea environment. During the last rapid decline of sea level in the late Oligocene, erosion occurred in the southern and western parts of the Nan'an Basin. The unconformity on the seismic profile expressed moderate to low frequency, moderate to high amplitude, and a continuous reflection (Figs. 3–5), which was identified as reflection T₄. The early Miocene sequence from drilling Well DH-1X can be divided into two cycles of sea level rise and fall, which represent the lower and upper parts of SQ2. The sedimentary facies

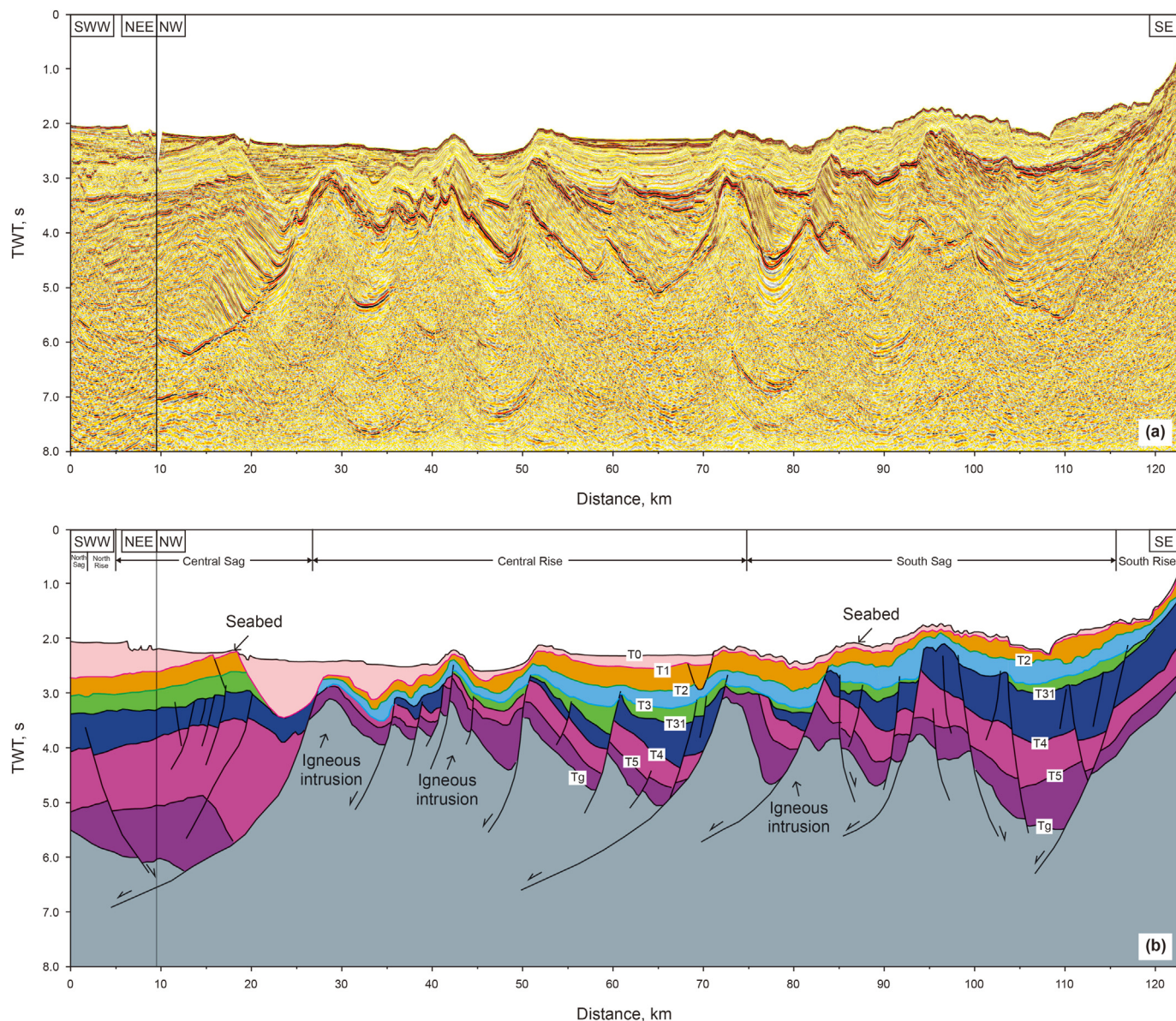


Fig. 3. Multichannel seismic reflection profile (a) and its interpretation (b). See Fig. 1b for location.

are typical of shore sands and mud. The lower tract consists of shallowing upward delta and foreshore deposits; the transgressive tract is composed of degraded parasequences, including shore sands and shale; and the high stand tract is dominated by shallow marine sand and mud, as well as mudstone.

SQ3 is the lower Lizhun Formation sequence. The sequence has seismic characteristics of moderate amplitude, moderate frequency, and a continuous reflection. Top truncation, concordance, bottom onlap, and downlap occurred. The sequence varies in thickness throughout the basin, with a maximum thickness of 2000–2800 m in the northern sag. Well DH-1X revealed that SQ3 was dominated by shallow marine facies.

SQ4 is located above the upper Lizhun Formation over reflector T₃. SQ4 has a moderate amplitude and continuous reflection (Figs. 3–6). The sequence was dominated by shallow marine facies, and thick carbonate platform sequences occurred in the uplift of the basin. It has two composite waves. A large sea level drop of 120 m is thought to have occurred at middle Miocene (Haq et al.,

1987; Yao et al., 2005; Lü et al., 2013). SQ4 consists of lowerstand prograded and aggraded parasequence, and the transgression is a retrograde parasequence. The highstand system tract was characterized by the carbonate platform development stage. Wells Dua-1X and AM-1X encountered thick carbonate sequences during the middle Miocene (Fig. 8).

SQ5 is the Kunlun Formation during the latest middle Miocene. SQ5 consists of prograded sandstone and mudstone on the carbonate platform. SQ5 has a moderate amplitude and continuous reflection (Figs. 3–6). The sequences was dominated by shallow terrigenous facies. SQ5 consists of lowerstand prograded and aggraded terrigenous sequences, while the highstand system tract was characterized by the carbonate platform development stage (Fig. 8).

SQ6 is the Lower Guangya Formation and is characterized by moderate to high frequency, moderate to weak amplitude, and moderate continuous reflections (Figs. 3–6). It may be early Pliocene lower-energy terrigenous deposits. Drilling Well AM-1X

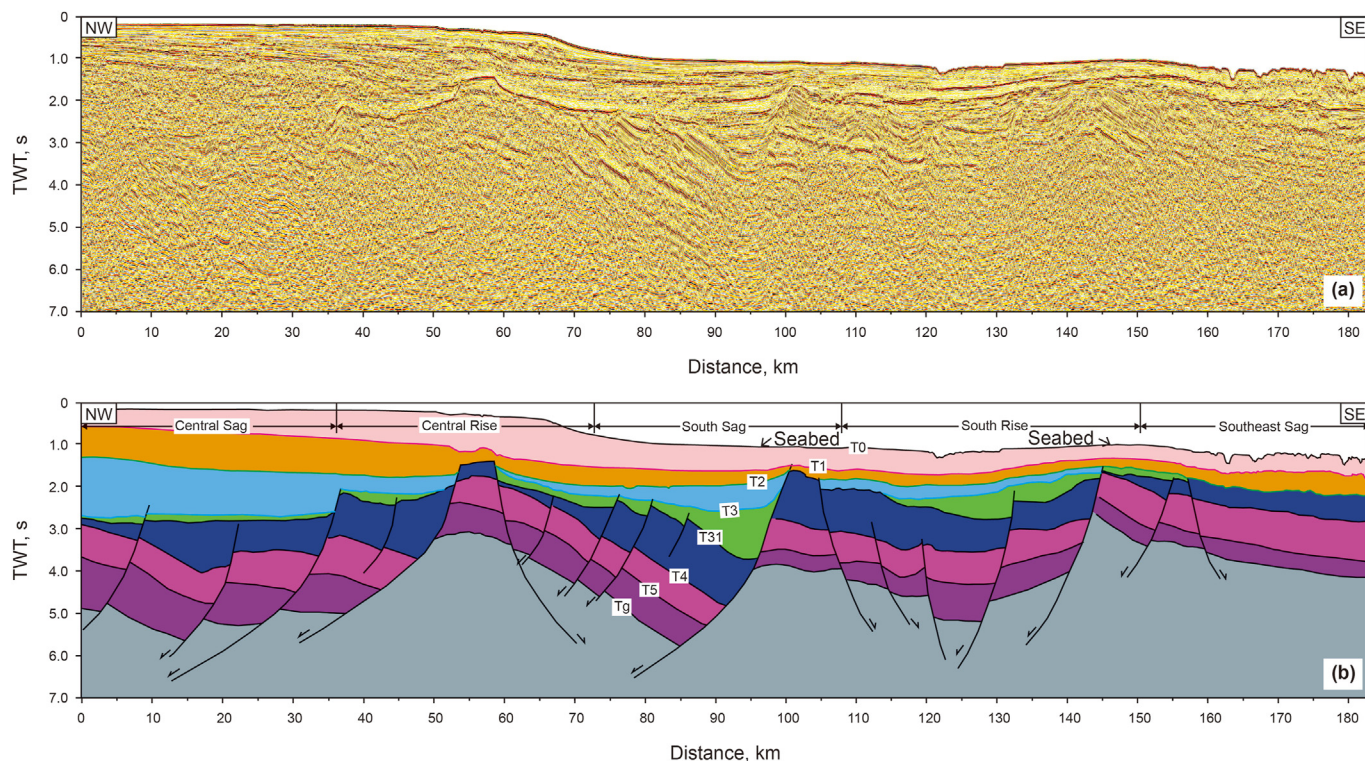


Fig. 4. Multichannel seismic reflection profile (a) and its interpretation (b). See Fig. 1b for location.

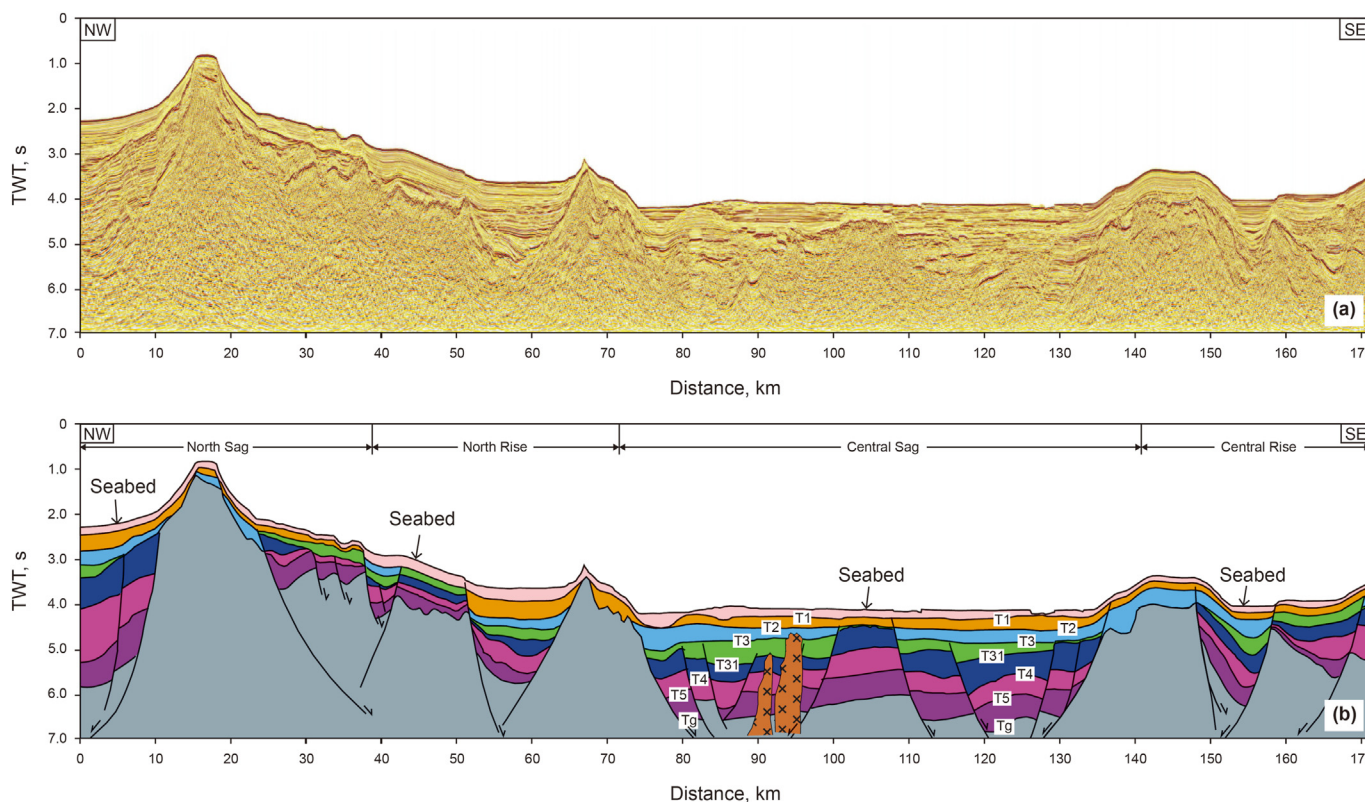


Fig. 5. Multichannel seismic reflection profile (a) and its interpretation (b). See Fig. 1b for location.

reveals that SQ6 consists of transgressive hemipelagic and high-stand tracts with prograded shallow marine and hemipelagic facies.

The lack of lowerstand system tract strata may lead to shelf uplift and bypass the continental slope, so the lowerstand system tract is

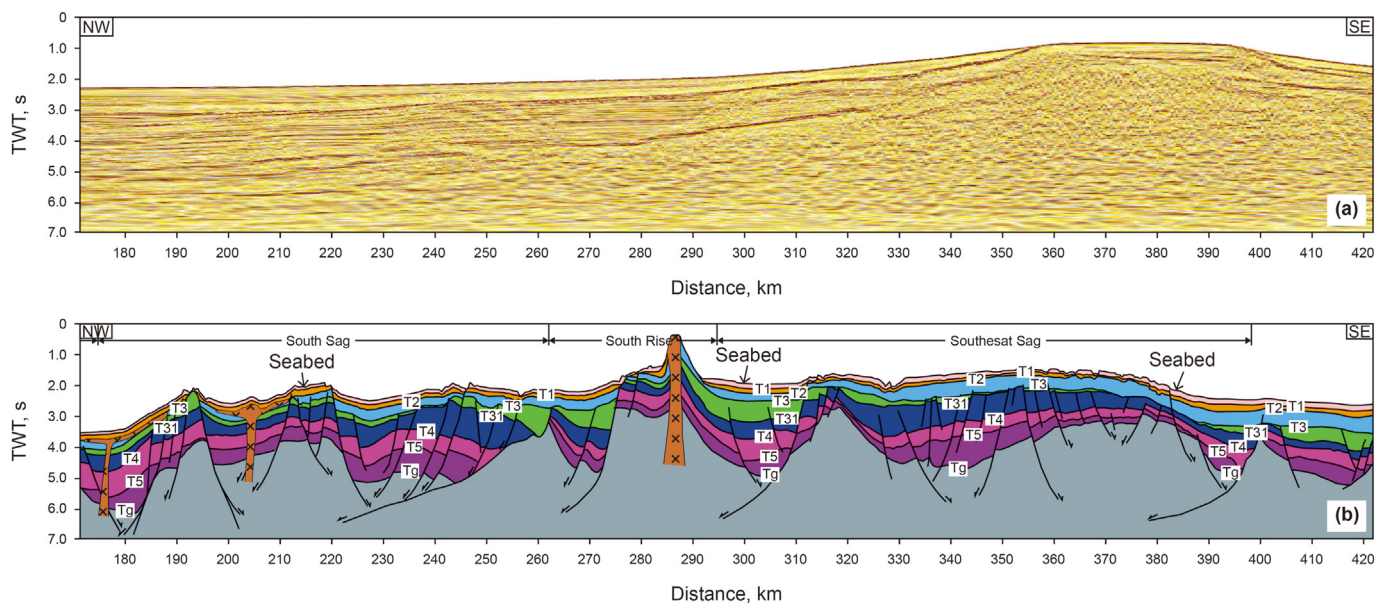


Fig. 6. Multichannel seismic reflection profile (a) and its interpretation (b). See Fig. 1b for location.

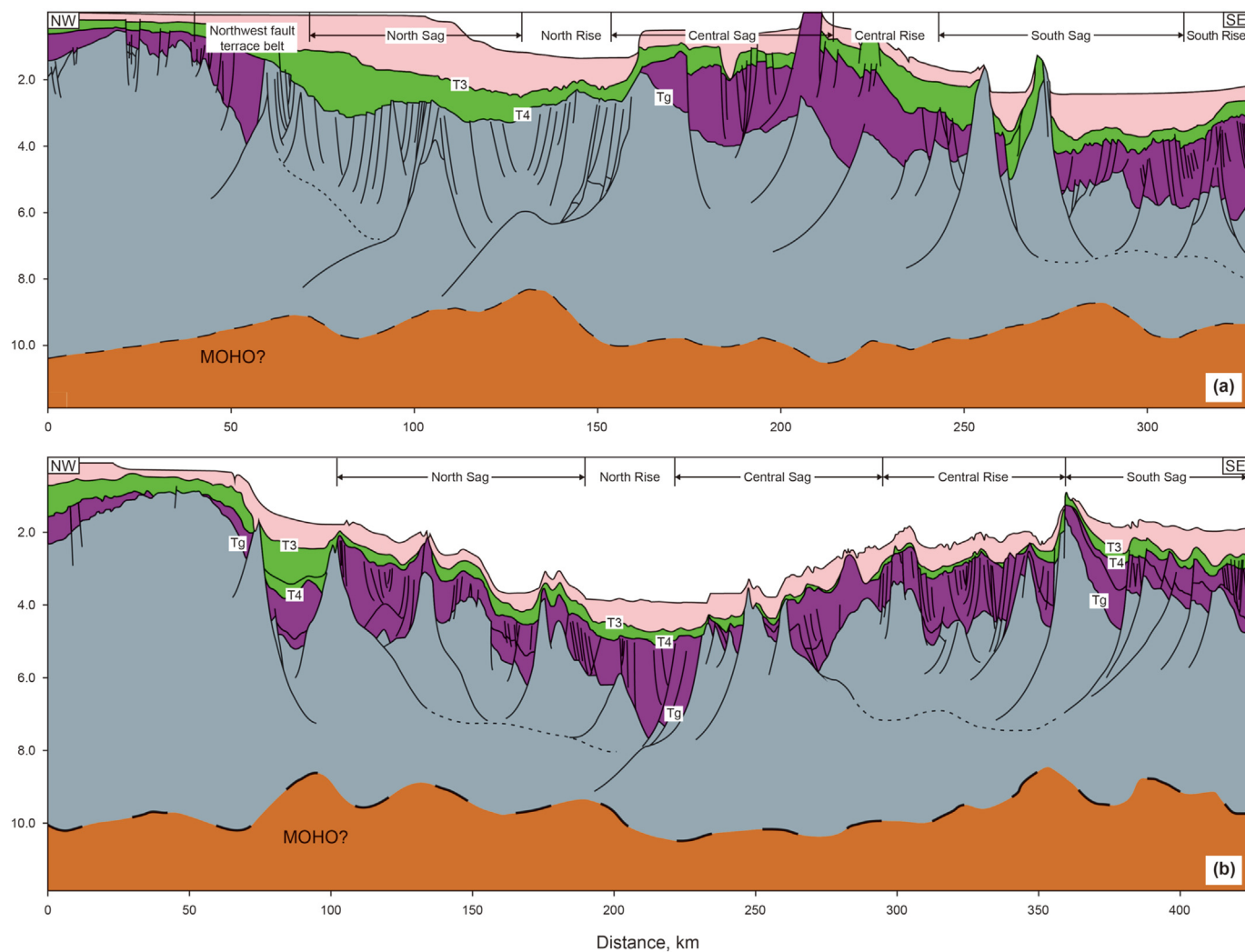


Fig. 7. The rifting graben across Nan'an Basin interpreted from the seismic profiles. (a) Interpretation of multichannel seismic reflection profile and (b) interpretation of seismic profile. See Fig. 1b for locations (modified from Franke et al., 2014).

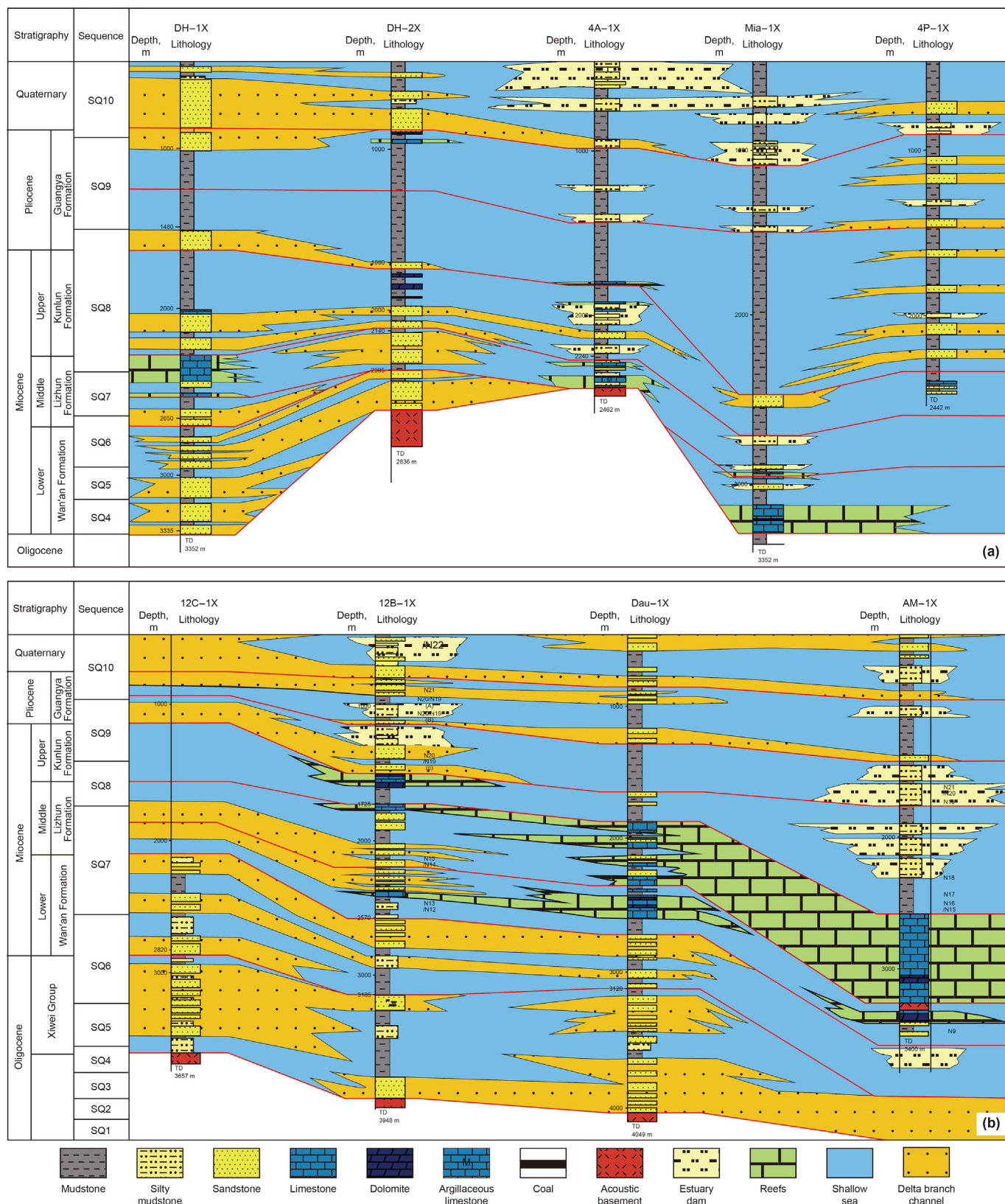


Fig. 8. (a) Geological sedimentary section across Wells DH-1X, DH-2X, 4A-1X, Mia-1X, and 4P-1X. (b) Geological section across Wells 12C-1X, 12B-1X, Dau-1X, and AM-1X. See Fig. 1b for well locations.

dominated by a deep-water turbidity channel system and mass transport deposits. The transgressive tract deposited a thick shallow marine shale, while the highstand system tract was characterized by a carbonate platform and deep sea development stage (Fig. 8).

SQ7 is the upper Guangya Formation and is characterized by moderate to high frequency, moderate to strong amplitude, and continuous reflections (Figs. 3–6). Drilling Well AM-1X revealed that SQ7 consists of transgressive hemipelagic and highstand system tracts of prograded shallow marine and hemipelagic facies. The lack of lowerstand system tract strata could indicate shelf uplift and bypass on the continental slope.

SQ8 is a Quaternary shelf to deep marine sequence that differentiates the shallow marine sequence in the west from the deep marine sequence in the east. Shallow marine mud was dominant in the western part of the basin, a shelf margin delta was distributed in the centre of the basin, and hemipelagic bioclastic clay and turbidites occurred on the continental slope (Figs. 3–6).

4. Tectonics of Nan'an Basin

4.1. Structural units

Nan'an Basin is characterized by a union rifting tectonic feature during the Cenozoic. The northern and southern boundaries are characterized by southeast- and northwest-dipping normal faults (Figs. 3–7, 9). The tectonic units of the basin consist of NE-SW-striking half-grabens and horsts, which were filled by a large number of rifting sequences (Fig. 1b). The boundary between the Nan'an and Zengmu Basins was separated by normal faults and an active magmatic uplift zone (Figs. 1b and 7a).

Two groups of faults with NE/NNE and NW strikes controlled the second structural units in Nan'an Basin (Fig. 1b). NE- and NNE-striking faults divided the main depressions and rises, while NW-striking faults have confined the west sag, shelf and slope geomorphology. The faults that occurred in Nan'an Basin were usually less than 200 km. The fault's throw could be 3 km. By combining the fault geometry and sedimentary evolution, Nan'an Basin has been divided into seven structural units: north sag, north rise,

central sag, central rise, south sag, south rise, and southeast sag.

The northern sag consists of a north fault terrace and a north-dipping half-graben (Figs. 6 and 7). It was controlled by NE-SW basement faults. The sequence above reflector T_5 is 6000–9000 m thick, and the maximum thickness is over 10000 m. Its acoustic basement trended to southward. The sedimentary centre is located in the southeast. Cover sequences increased the thickness of the strata to the southeast and had a well-developed sigmoid progradation configuration. Yao et al. (2005) suggested that depression in the west could be a part of the northern sag. It was controlled by NNE- and ENE-trending basement faults. The sag overlapped on the Xibei Fault terrace in the south-eastward direction.

Strikes in the northern rise trended NE-SW with fault terraces, which consist of several terraces that decrease to the southeast. Cenozoic strata over reflector T_5 had a thickness of 2000–5000 m. The sequence above reflector T_5 is 2700–7000 m thick, and the maximum thickness is over 9000 m. The rise extended to the slope in the eastward direction (Fig. 6).

The central sag is a NE-SW striking graben in the centre of the basin and is retained by the north and south rises (Figs. 6–9). It consists of two concordant faults. It has Cenozoic strata with a thickness ranging from 6000 to 9000 m, and a maximum thickness of 12000 m. The structural rise in the sag is more than 4000 m. Rifting sequences were formed as an anticline. The cover sequences were dominated by the sigmoid configuration in the south-eastward direction.

The central rise has NE-SW trend which was consisted of a narrow basement horst. The sequence above reflector T_5 is 4000–6000 m thick, and the maximum thickness is over 9000 m. The rise extended to the slope in the eastward direction (Figs. 6 and 7).

The southern sag is located south of the basin and consists of two half grabens. It has Cenozoic strata with a thickness of 6000–9000 m and a maximum thickness of 12000 m (Fig. 7). The structural rise in the depression is more than 4000 m. Rifting sequences were formed as an anticline. The cover sequences were dominated by the sigmoid configuration in the south-eastward direction.

The southern rise is characterized by NE detached faults. The sag in the rise consists of several half grabens. The rifting fault block is a south-rise-cropped seafloor or is covered by thin sediments. Narrow uplift separated the central and southern sags. The acoustic basement of the southern sag dipped northwest. The total sedimentary sequences have a thickness of 2000–4000 m (Fig. 7).

The southeast sag is the largest depression, covering 3.0×10^4 km², but the rifting sequences include several small-scale half-grabens filled in with thin rifting sequences. The total Cenozoic strata is 10.4 km thick. Zengmu Basin was separated by a backward faulting horst and a high volcanic intrusion (Fig. 7). The late Miocene to Quaternary geomorphology increased the water depth in the Zengmu Basin but was intruded by volcanic seamounts. The sag consisted of several small half-grabens covered by terrigenous sediments.

4.2. Structural layers

Seismic reflectors T_3 , T_5 , and T_g were apparent regional unconformities, which could be related to three important tectonic layers: the end of the rifting unconformity (reflector T_3), onset of the rifting unconformity in the Eocene (E2/E3), and the initial rifting unconformity (reflector T_5). The end of the rifting unconformity (reflector T_g) is a very important surface in Nan'an Basin (Franke et al., 2014).

Based on the three main unconformities, three tectonic layers were divided in the cover strata of the sedimentary basin

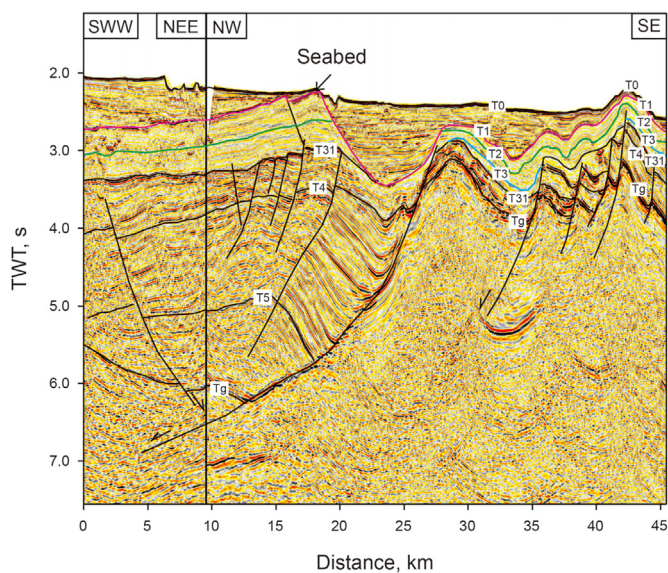


Fig. 9. Typical rifting fractures and half-graben structures are well developed in Nan'an Basin, interpreted from the multichannel seismic reflection profile L7. See Fig. 1b for location.

(Figs. 4–7). The lower tectonic layer indicates the presence of fluvial lacustrine facies between seismic reflectors T_4 and T_6 . It was early half-graben rifting fill after compressional uplift. It was limited to the east and northeast regions of the basin. However, this sedimentary layer in the deepest depression was not encountered due to the vague seismic facies and its large thickness (Fig. 7).

The middle tectonic layer included well-deformed sedimentary strata, which represent the very important rifting stage sequence between reflectors T_3^1 and T_4 . The sequences included the Wan'an and Lizhun Formations. The lower part of the sequence is half-graben fill and terrigenous sill drape from the shelf to the continental slope. The upper sequence has well-developed carbonate platforms (Lü et al., 2013; Wu et al., 2016). The sequence varied from lacustrine to shallow water and deep-water sedimentary facies but was dominated by delta, littoral, and shallow marine facies. The Wan'an movement in the late to middle Miocene reformed the middle tectonic layer. Faulted anticlines, tilted blocks, and uplifting erosion have been found in the basin.

The upper tectonic layer is the thickness of the continental shelf terrigenous sedimentary facies. The sequence includes the Kunlun, Guangya, and Quaternary Formations. It occurs in the S-style reflection from the shelf to the slope and has a well-developed large progradational structure. The sequence has a high-amplitude reflection, good continuity, and gentle occurrence. Shallow water carbonate platforms at the shelf margin were well developed.

4.3. Tectonic evolution

Nan'an Basin is a westward extension of the Southwest Subbasin. Acoustic basements in Wan'an Basin are composed of a Jurassic-Cretaceous volcanic arc (Matthews et al., 1997; Liu et al., 2004; Yan et al., 2006; Yu et al., 2018). The onset of rifting in the basin could be in the late Cretaceous (Fig. 10). The early rifting sequence encountered by the drilling well could be Eocene and Oligocene Lacustrine facies (Fig. 10b and c). Early erosion and deplanation produced a thick terrestrial facies filled the NE-striking graben.

The last rifting stage extended to the middle Miocene (Fig. 10d). The basin experienced short-term uplift and erosion during the early to middle Miocene. Subsequently, the two rifting centres were distributed in the northern and southern sags. The sags deposited terrestrial lacustrine, fluvial, and transitional facies. Since the early Miocene, the rifting graben basin united together and encompassed a large delta and shallow carbonate platforms. During the middle Miocene, Nan'an Basin continued to subside, and deep-water sedimentation occurred in the east. A late to middle Miocene tectonic reversal occurred and led to an important unconformity in Wan'an Basin, similar to the movement in the Zengmu Basin.

The post-rifting sequence during the late Miocene to Quaternary (N_3^1 -Q) filled the thermal subsidence stage, which produced regional subsidence and formed a shallow marine to deep marine environment (Fig. 10e). The shelf margin delta and deep-water sedimentary system were well developed in the east of the Nan'an Basin.

5. Discussion

5.1. A rift basin or pull-apart basin?

The debate surrounding the features of Nan'an Basin has long been drawn out. Some studies suggest that giant strike-slip faults existed and propose that the basin has a pull-apart origin (Liu et al., 2004; Yao et al., 2008). However, other studies proposed that Nan'an Basin was characterized by a typical rift basin structure based on seismic profiles (Matthews et al., 1997; Franke et al.,

2014). An aborted rifting trough is the early evolution stage of the Southwest Subbasin (Song et al., 2019; Dong et al., 2020). The seismic transects across the basin indicate that Nan'an Basin was a rift basin from the Eocene to Miocene (Matthews et al., 1997; Hutchison, 2004; Franke et al., 2014). Previous studies proposed that continental crustal extension occurred along the western segments. Franke et al. (2014) indicated that extension can be transferred over a wide range, and was mainly controlled by lateral flow in the ductile crustal layers. The lower-angle reflections of Nan'an Basin are interpreted as inactive low-angle normal faults (detachment faults). This type of fault is persevered in Nan'an Basin (Franke et al., 2014). Closer to the coast and underneath the shelf, the faults solidify at detachment surfaces, which is located below individual rift basins that are separated by horst blocks (Figs. 7 and 8). These faults are characterized by highly thinning of the crust and the presence of major ductile shear zones acting as a detachment fault in the middle crustal layer. According to Lavier and Manatschal (2006), these detachment faults provide accommodation space for differential extension between the upper crust, the lower crust, and upper mantle, which is accompanied by little uplift of the rift flanks and subsidence in the hanging wall.

When oceanic crust occurred in the Southwest Subbasin, the rifting system was still active in extension mode in Nan'an Basin. Continued extension in the western rift led to extra extension and subsequent transition to the thinning mode. The second rift phase is different from the wedge-shaped fill in the rift basins which near the Southwest Subbasin. Here, thinning crustal on seismic profile is most distinct feature, but we believe that there is considerable variability along the continent ocean transition zone; therefore, inexact conjugate profiles may lead to ambiguous interpretations (Franke, 2013; Franke et al., 2014). This interpretation may not consistent with fact that the rifting mode observed in South China Sea did not lead to a typical simple-shear structure (Dong et al., 2020).

Nan'an Basin has a long history of rifting deformation. It can be divided into three stages: (1) Late Cretaceous to Eocene initial rifting; (2) Eocene to Oligocene rifting that induced the main grabens and rises; (3) Miocene rifting. Lü et al. (2013) believed that rifting in the middle Miocene was mainly confined to late, and the pre-existing topography was filled by faulting and subsequent carbonate growth, as well as sea-level changes. According to their report, no significant faulting activity has occurred since the late Miocene. The third stage extension is relatively minor in the line of the section, and extension ceased at the end of the late Miocene (Matthews et al., 1997; Lee et al., 2001; Li et al., 2014a; Li et al., 2014b). Figs. 5–7 show a single fault-bounded basin with both the upper Miocene Wan'an Formation and the middle Miocene Lizhun Formation. Significant faulting in the middle Miocene sequence occurred at the southwest SCS margin. The seismic profiles (Figs. 5–7) illustrate that the unconformities in the basins adjacent to the South China Sea were broken up and widespread, as is the 10.5 Ma spreading centre. The early Oligocene unconformity marks the end of the second rifting stage. Based on the timing of deformation in the basins of the southern SCS margin, the upper Miocene Wan'an Formation is usually considered a post-rift sequence, while a new phase of rifting stage was identified in the middle Miocene Lizhun Formation, and the late Miocene Kunlun Formation between 15.5 Ma and 10.4 Ma (Lunt, 2019, Fig. 2). The two rifting phase unconformities was separated by the post-rifting Wan'an Formation (Fig. 2). The main synrift phase lasted from the Eocene to the Oligocene. In Nan'an Basin, there was a period of post-rift subsidence (late Oligocene-early Miocene), followed by middle Miocene extension, which ended at approximately 10.5 Ma.

Nan'an Basin is characterized by typical rift basin structures (Figs. 3–7). The aborted rifting trough is the early evolution stage of

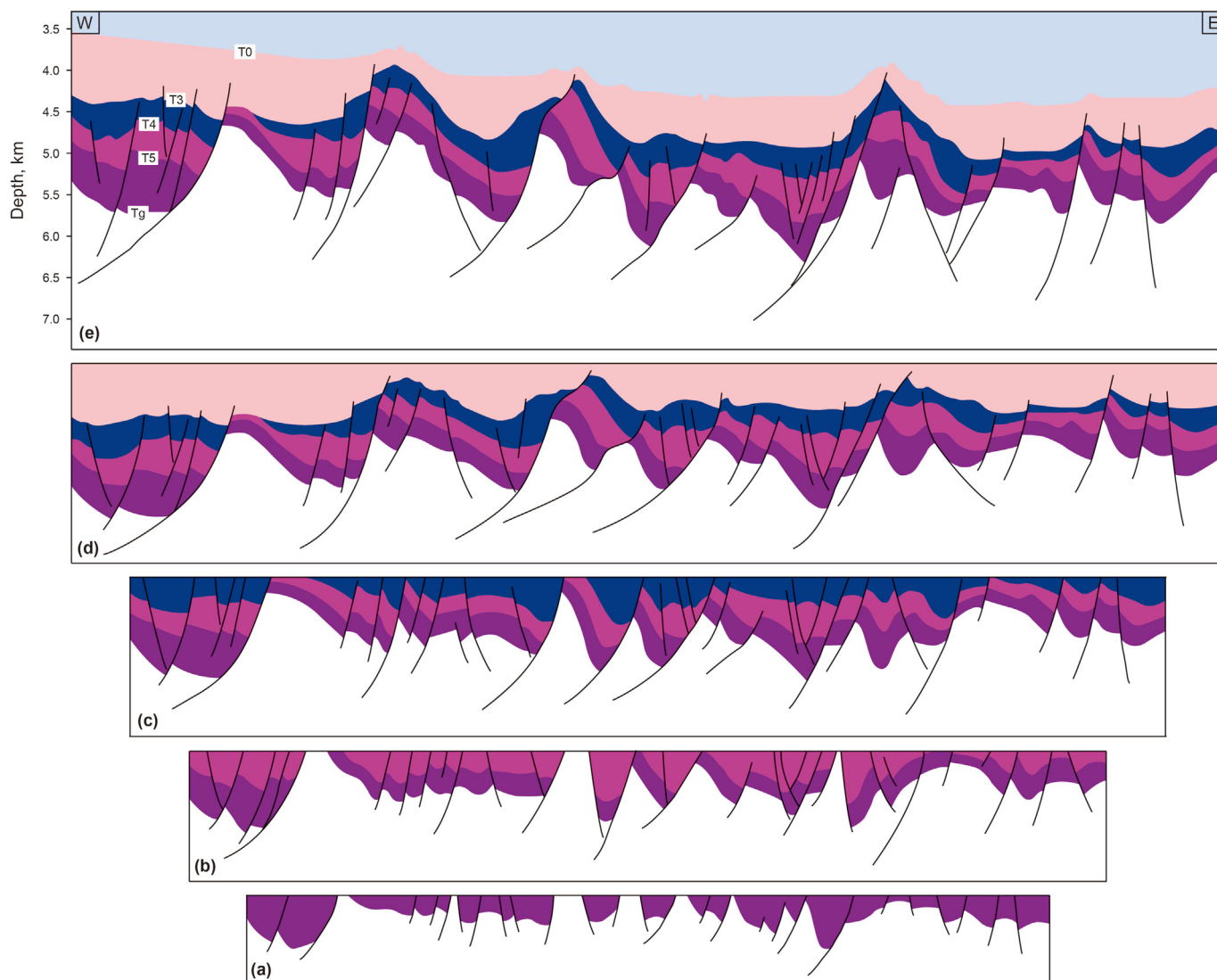


Fig. 10. Tectonic evolution model of the Nan'an Basin, South China Sea since the Eocene. (a): Erosion acoustic basement before the Eocene, (b): Early rifting sequences during the Eocene, (c): Early rifting sequences during the Oligocene, (d): Late rifting sequences during the early and middle Miocene, (e): Post-rifting marine facies sequences since the late Miocene.

the Southwest Subbasin (Dong et al., 2016; Song et al., 2019; Taylor and Hayes, 1980). The seismic transects across the basin indicate that Nan'an Basin expresses a rift basin from the Eocene to Miocene (Franke et al., 2014; Matthews et al., 1997). Previous studies proposed that continental crustal extension occurred along the western segments. These lower-angle reflections of Nan'an Basin are interpreted as inactive low-angle normal faults (detachment faults) (Liang et al., 2019; Schlüter et al., 1996). These types of faults are preserved in Nan'an Basin (Franke et al., 2014).

A typical listric fault style occurred along the western margin of the South China Sea (Franke et al., 2014, Fig. 9). Therefore, concordance of Nan'an Basin's Southwest Subbasin indicates no giant strike-slip movement along the southwest margin. Nan'an Basin at the tip of the Southwest Subbasin is characterized as an extensional basin in which the main depression-defining faults have not experienced major strike-slip displacements.

5.2. North-south strike slip movement and evolution of the western south China sea margin

Although some studies have argued that a N-S strike-slip fault existed in Nan'an Basin, no direct evidence was found in the seismic data that supports this proposition (Figs. 8 and 9). Yao et al. (2005) emphasized that the Wandong left-lateral striking-slip Fault was active from the Eocene to the middle Miocene (Yao et al., 2008). This fault induced a NE-trending striking-slip fault, suggesting that the faults controlled the rifting depressions. In fact, there was no apparent N-S direction fault movement along the shelf break strike-slip faults. Seismic data show that the main fault systems were in a NE-SW direction (Fig. 1b). Shallow-water carbonate platforms were distributed along the NE-SW striking direction, which was controlled by the main NE direction depressions. Matthews et al. (1997) also stated that there was no direct evidence in the seismic datasets for Paleogene strike-slip displacement. Therefore, we consider that minor transfer faults with an approximately NNE-SSW trend are the segments of the major NE-SW trending rift defining faults.

On the contrary, some evidences suggested that similarly striking slip faults occurred immediately onshore and offshore (Rangin et al., 1995). They suggested the exist of the left-lateral movement in the rifting stage, and onset of right-lateral movement during the early Neogene between the Nan'an Basin and Southwest Subbasin. In response to the opening of the Southwest Subbasin, a gradual transgression occurred in the Nan'an basin, which resulted in the dominance of lower Miocene marine siliciclastic sequences (Matthews et al., 1997; Yao et al., 2008). As transgression continued, a gradual deepening took place across the basin depocenters and widespread carbonate deposition commenced (Li et al., 2014a; Lee et al., 2001). During the late middle Miocene, a relative sea-level lowstand temporarily interrupted carbonate platform development. The associated unconformity pronouncedly truncates the underlying formations and marks a distinct decrease in rifting. The steep geomorphology and gravity anomaly induced by the shelf margin carbonate platform, but not north-south strike slip movement.

6. Conclusions

Nan'an Basin is a typical rift basin. It is an aborted rifting trough compared to the occurrence of oceanic crust in the Southwest Subbasin. The extension can be transferred across a wide range, which is mainly controlled by lateral flow in the ductile crustal layers. Major low-angle reflections of Nan'an Basin are interpreted as inactive low-angle normal faults (detachment faults). Nan'an Basin is characterized by extensive crust thinning and the existence of major ductile shear zones, which act as detachments at the middle crustal levels.

The tectonic evolution of Nan'an Basin has been divided into four stages since the late Cretaceous: (1) initial rifting from late Cretaceous to Eocene; (2) rifting that induced the main grabens and rises from Eocene to Oligocene; (3) rifting from early to middle Miocene; and (4) shelf and deep marine development stage from late Miocene to Quaternary.

This study shows that there are no apparent NS strike-slip faults in the central Nan'an Basin. Minor transfer faults with an approximately NNE-SSW trend are interpreted to be segments of the major NE-SW trending rift defining faults. The steep geomorphology was induced by shallow water Miocene carbonate platform development along the NS direction shelf break.

Acknowledgements

The authors are grateful to Guangzhou Marine Geological Survey (GMGS) for their permission to release seismic data and the subsurface data. This research was financially supported by Natural Science Foundation of China (U1701245, No. 91228208), CGS project (DD20190213), and CNPC project (kt 2021-02-02).

References

- Barckhausen, U., Engels, M., Franke, D., et al., 2014. Evolution of the South China Sea: revised ages for breakup and seafloor spreading. *Mar. Petrol. Geol.* 58, 599–611. <https://doi.org/10.1016/j.marpetgeo.2014.02.022>.
- Clift, P., Lee, G.H., Anh Duc, N., et al., 2008. Seismic reflection evidence for a Dangerous Grounds miniplate: No extrusion origin for the South China Sea. *Tectonics* 27 (3), 159–174. <https://doi.org/10.1029/2007TC002216>.
- Cullen, A., Reemst, P., Henstra, G., et al., 2010. Rifting of the south China sea: new perspectives. *Petrol. Geosci.* 16 (3), 273–282. <https://doi.org/10.1144/1354-079309-908>.
- Ding, W.W., Franke, D., Li, J.B., Steuer, S., 2013. Seismic stratigraphy and tectonic structure from a composite multi-channel seismic profile across the entire Nansha Waters. South China Sea. *Tectonophy.* 582, 162–176. <https://doi.org/10.1016/j.tecto.2012.09.026>.
- Dong, M., Wu, S.G., Zhang, J., 2016. Thinned crustal structure and tectonic boundary of the Nansha Block, southern South China Sea. *Mar. Geophys. Res.* 37 (4), 281–296. <https://doi.org/10.1007/s11001-016-9290-3>.
- Dong, M., Zhang, J., Brune, S., et al., 2020. Quantifying post-rift lower crustal flow in the northern margin of the South China Sea. *J. Geophys. Res. Solid Earth* 125 (2), e2019JB018910. <https://doi.org/10.1029/2019JB018910>.
- Dung, B.V., Tuan, H.A., Van Kieu, N., et al., 2018. Depositional environment and reservoir quality of Miocene sediments in the central part of the Nam Con Son basin, Southern Vietnam shelf. *Mar. Petrol. Geol.* 97, 672–689. <https://doi.org/10.1016/j.marpetgeo.2018.05.004>.
- Franke, D., 2013. Rifting, lithosphere breakup and volcanism: comparison of magma-poor and volcanic rifted margins. *Mar. Petrol. Geol.* 43, 63–87. <https://doi.org/10.1016/j.marpetgeo.2012.11.003>.
- Franke, D., Savva, D., Pubellier, M., et al., 2014. The final rifting evolution in the South China Sea. *Mar. Petrol. Geol.* 58, 704–720. <https://doi.org/10.1016/j.marpetgeo.2013.11.020>.
- Gao, J., Wu, S., McIntosh, K., et al., 2016. Crustal structure and extension mode in the northwestern margin of the South China Sea. *G-cubed* 17 (6), 2143–2167. <https://doi.org/10.1002/2016GC006247>.
- Hall, R., 2002. Cenozoic geological and plate tectonic evolution of SE Asia and the SW Pacific: computer-based reconstructions, model and animations. *J. Asian Earth Sci.* 20 (4), 353–431. [https://doi.org/10.1016/S1367-9120\(01\)00069-4](https://doi.org/10.1016/S1367-9120(01)00069-4).
- Haq, B.U., Hardenbol, J.A.N., Vail, P.R., 1987. Chronology of fluctuating sea levels since the Triassic. *Science* 235 (4793), 1156–1167. <https://doi.org/10.1126/science.235.4793.1156>.
- Hutchison, C.S., 2004. Marginal basin evolution: the southern South China Sea. *Mar. Petrol. Geol.* 21 (9), 1129–1148. <https://doi.org/10.1016/j.marpetgeo.2004.07.002>.
- Lavier, L., Manatschal, G., 2006. A mechanism to thin the continental lithosphere at magma-poor margins. *Nature* 440 (7082), 324–328. <https://doi.org/10.1038/nature04608>.
- Lee, G.H., Lee, K., Watkins, J.S., 2001. Geologic evolution of the Cuu long and Nam Con Son basins, offshore southern vietnam, south China sea. *AAPG Bull.* 85 (6), 1055–1082. <https://doi.org/10.1306/8626CA69-173B-11D7-8645000102C1865D>.
- Li, C.F., Xu, X., Lin, J., et al., 2014a. Ages and magnetic structures of the South China Sea constrained by deep tow magnetic surveys and IODP Expedition 349. *G-cubed* 15 (12), 4958–4983. <https://doi.org/10.1002/2014GC005567>.
- Li, L., Clift, P.D., Stephenson, R., et al., 2014b. Non-uniform hyper-extension in advance of seafloor spreading on the vietnam continental margin and the SW South China Sea. *Basin Res.* 26 (1), 106–134. <https://doi.org/10.1111/bre.12045>.
- Liang, Y., Delescluse, M., Qiu, Y., et al., 2019. Décollements, detachments, and rafts in the extended crust of Dangerous Ground, South China Sea: the role of inherited contacts. *Tectonics* 38 (6), 1863–1883. <https://doi.org/10.1029/2018TC005418>.
- Liu, H., Yan, P., Zhang, B., et al., 2004. Role of the wan-Na fault system in the western Nansha islands (southern South China Sea). *J. Asian Earth Sci.* 23 (2), 221–233. [https://doi.org/10.1016/S1367-9120\(03\)00121-4](https://doi.org/10.1016/S1367-9120(03)00121-4).
- Lü, C., Wu, S., Yao, Y., et al., 2013. Development and controlling factors of Miocene carbonate platform in the Nam Con Son Basin, southwestern south China sea. *Mar. Petrol. Geol.* 45, 55–68. <https://doi.org/10.1016/j.marpetgeo.2013.04.014>.
- Lunt, P., 2019. A new view of integrating stratigraphic and tectonic analysis in South China Sea and north Borneo basins. *J. Asian Earth Sci.* 177, 220–239. <https://doi.org/10.1016/j.jseas.2019.03.009>.
- Madon, M., Kim, C.L., Wong, R., 2013. The structure and stratigraphy of deepwater Sarawak, Malaysia: implications for tectonic evolution. *J. Asian Earth Sci.* 76, 312–333. <https://doi.org/10.1016/j.jseas.2013.04.040>.
- Matthews, S.J., Fraser, A.J., Lowe, S., et al., 1997. Structure, stratigraphy and petroleum geology of the SE Nam Con Son Basin, offshore Vietnam. *Geol. Soc. Lond. Spec. Publ.* 126 (1), 89–106. <https://doi.org/10.1144/GSL.SP.1997.126.01.07>.
- Morley, C.K., 2002. A tectonic model for the Tertiary evolution of strike-slip faults and rift basins in SE Asia. *Tectonophysics* 347 (4), 189–215. [https://doi.org/10.1016/S0040-1951\(02\)00061-6](https://doi.org/10.1016/S0040-1951(02)00061-6).
- Morley, C.K., 2016. Major unconformities/termination of extension events and associated surfaces in the South China Seas: review and implications for tectonic development. *J. Asian Earth Sci.* 120, 62–86. <https://doi.org/10.1016/j.jseas.2016.01.013>.
- Peng, X., Shen, C., Mei, L., et al., 2019. Rift–drift transition in the dangerous grounds, south China sea. *Mar. Geophys. Res.* 40 (2), 163–183. <https://doi.org/10.1007/s11001-018-9353-8>.
- Qiu, Y., Zeng, W.J., Li, T.G., 2005. Fracture systems and their tectonic significance in the central and southern parts of the South China Sea. *Geotect. Metallogenia* 29 (2), 166–175. <https://doi.org/10.3969/j.issn.1001-1552.2005.02.002> (in Chinese).
- Rangin, C., Klein, M., Roques, D., et al., 1995. The Red river fault system in the Tonkin Gulf, Vietnam. *Tectonophy.* 243 (3–4), 209–222. [https://doi.org/10.1016/0040-1951\(94\)00207-P](https://doi.org/10.1016/0040-1951(94)00207-P).
- Savva, D., Pubellier, M., Franke, D., et al., 2014. Different expressions of rifting on the South China Sea margins. *Mar. Petrol. Geol.* 58, 579–598. <https://doi.org/10.1016/j.marpetgeo.2014.05.023>.
- Schlüter, H.U., Hinz, K., Block, M., 1996. Tectono-stratigraphic terranes and detachment faulting of the south China sea and sulu sea. *Mar. Geol.* 130 (1–2), 39–78. [https://doi.org/10.1016/0025-3227\(95\)00137-9](https://doi.org/10.1016/0025-3227(95)00137-9).
- Song, T., Li, C.F., Wu, S., et al., 2019. Extensional styles of the conjugate rifted margins of the South China Sea. *J. Asian Earth Sci.* 177, 117–128. <https://doi.org/10.1016/j.jseas.2019.03.008>.
- Sun, Z., Zhao, Z.X., Zhou, D., et al., 2011. The stratigraphy and the sequence architecture of the basins in Nansha region. *Earth Sci. J. China Univ. Geosci.* 36 (5),

- 798–806. <https://doi.org/10.3799/dqkx.2011.082> (in Chinese).
- Tapponnier, P., Peltzer, G., Le Dain, A.Y., et al., 1982. Propagating extrusion tectonics in Asia: new insights from simple experiments with plasticine. *Geology* 10 (12), 611–616. [https://doi.org/10.1130/0091-7613\(1982\)10<611:PETIAN>2.0.CO;2](https://doi.org/10.1130/0091-7613(1982)10<611:PETIAN>2.0.CO;2).
- Taylor, B., Hayes, D.E., 1980. The tectonic evolution of the south China basin//Hayes D E. The tectonic and geologic evolution of southeast asian seas and islands: Part 2. *Am. Geophys. Union* 23–56.
- Wu, J.M., 1997. The strike-slip fracture system and the convolute structure of Zengmu basin in Southwestern South China sea. *Geol. Res. South China Sea* 9, 54–66 (in Chinese).
- Wu, S., Zhang, X., Yang, Z., et al., 2016. Spatial and temporal evolution of Cenozoic carbonate platforms on the continental margins of the South China Sea: response to opening of the ocean basin. *Interpretation* 4 (3), SP1–SP19. <https://doi.org/10.1190/INT-2015-0162.1>.
- Yan, P., Deng, H., Liu, H., et al., 2006. The temporal and spatial distribution of volcanism in the South China Sea region. *J. Asian Earth Sci.* 27 (5), 647–659. <https://doi.org/10.1016/j.jseas.2005.06.005>.
- Yan, Q., Shi, X., Castillo, P.R., 2014. The late Mesozoic–Cenozoic tectonic evolution of the South China Sea: a petrologic perspective. *J. Asian Earth Sci.* 85, 178–201. <https://doi.org/10.1016/j.jseas.2014.02.005>.
- Yao, Y.J., Xia, B., Xu, X., 2005. Tectonic evolution of the main sedimentary basins in southern area of the South China Sea. *Geol. Res. South China Sea* 17, 1–11 (in Chinese).
- Yao, Y.J., Wu, N.Y., Xia, B., et al., 2008. Petroleum geology of the Zengmu Basin in the southern south China sea. *Chin. Geol.* 35 (3), 503–513. <https://doi.org/10.3969/j.issn.1000-3657.2008.03.015> (in Chinese).
- Yao, Y.J., Lü, C.L., Wang, L.J., et al., 2018. Tectonic evolution and genetic mechanism of the wan'an basin, southern south China sea. *Hai Yang Xue Bao* 40 (5), 62–74. <https://doi.org/10.3969/j.issn.0253-4193.2018.05.006> (in Chinese).
- Yu, J., Yan, P., Wang, Y., et al., 2018. Seismic evidence for tectonically dominated seafloor spreading in the Southwest Sub-basin of the South China Sea. *G-cubed* 19 (9), 3459–3477. <https://doi.org/10.3969/j.issn.0253-4193.2018.05.006>.
- Zhang, G., Qu, H., Zhang, F., et al., 2019. Major new discoveries of oil and gas in global deepwaters and enlightenment. *Acta Pet. Sin.* 40 (1), 1–34. <https://doi.org/10.7623/syxb201901001> (in Chinese).
- Zhu, L., Ma, Y., Cai, J., et al., 2022. Key factors of marine shale conductivity in southern China—Part II: the influence of pore system and the development direction of shale gas saturation models. *J. Petrol. Sci. Eng.* 209, 109516. <https://doi.org/10.1016/j.petrol.2021.109516>.